

Independent dimensional phase transition on a two-dimensional Kuramoto model with matrix coupling

Chongzhi Wang, Haibin Shao, and Dewei Li*

Department of Automation, Shanghai Jiao Tong University,

Key Laboratory of System Control and Information Processing, Ministry of Education of China, Shanghai Engineering Research Center of Intelligent Control and Management, Shanghai, 200240, China

(Dated: August 27, 2021)

The high-dimensional generalization of the one-dimensional Kuramoto paradigm has been an essential step in bringing about a more faithful depiction of the dynamics of real-world systems. Despite the multi-dimensional nature of the oscillators in these generalized models, the interacting schemes so far have been dominated by a scalar factor unanimously between any pair of oscillators that leads eventually to synchronization on all dimensions. As a natural extension of the scalar coupling befitting for the one-dimensional case, we take a tentative step in studying numerically and theoretically the coupling mechanism of 2×2 real matrices on two-dimensional Kuramoto oscillators. One of the features stemmed from this new mechanism is that the matrix coupling enables the two dimensions of the oscillators to separate their transitions to either synchronization or desynchronization which has not been seen in other high-dimensional generalizations. Under various matrix configurations, the synchronization and desynchronization of the two dimensions combine into four qualitatively distinct modes of position and motion of the system. We demonstrate that as one matrix is morphed into another in a specific manner, the system mode also switches correspondingly either through continuous or explosive transitions of the order parameters, thus mimicking a range of behaviors in information science and biology.

Autonomous behavior of large ensembles of interacting entities has been an observation captured both in the realms of nature and of artificial creations [1, 2]. Proposed as a mathematically-tractable model to address this fact and probably as the nontrivial many-body problem in its simplest form [3], the Kuramoto paradigm was thoroughly studied for the exemplary phenomena it induces on the all-to-all sinusoidally coupled one-dimensional oscillators on the unit circle [4–6]. Among other things, the synchronization phase transition hints at similar processes in many problems of physical or engineering background such as the Josephson junction arrays [3], the XY model with quenched randomness [7], and those of biological background [8, 9]. Due to this versatility in lower dimensions, the classic Kuramoto model was rapidly gaining generalizations in many ways possible, for which there is in particular, the high-dimensional Kuramoto model where the phase variables are replaced by unit vectors that are coupled proportionally to the sine of the vectors' displacement angle [10, 11]; or in a multi-layer setting, information of an oscillator spreads into different layers, and inter-layer as well as intra-layer interactions take place [12]. Regardless, a single scalar variable spans the parameter space that tunes the coupling strength for all dimensions where each eventually secures a synchronization, hence no discernable long-term behaviors are displayed thereon as long as the coupling is sufficiently strong.

If we revisit the generalization process and take the simplest possible multi-dimensional case to work with, for a three dimensional unit vector, the oscillator is left with two degrees of freedom that are fully described by the two angle variables in the sphere coordinates. In this Letter,

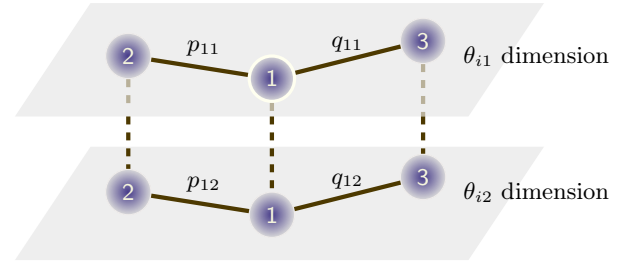


FIG. 1. *The matrix coupling mechanism.* Illustration of how the three oscillators and their dimensions are interacting, given that θ_1 is connected with θ_2 and θ_3 weighed by matrices $P = \begin{bmatrix} p_{11} & p_{12} \\ p_{21} & p_{22} \end{bmatrix}$ and $Q = \begin{bmatrix} q_{11} & q_{12} \\ q_{21} & q_{22} \end{bmatrix}$ respectively. Solid lines connect variables that are differenced before being acted on by the sine function, while dashed lines connect two dimensions of the same oscillator that are not explicitly interacting. By examining the dynamics of θ_{11} , one finds that the terms $\sin(\theta_{j1} - \theta_{11})$ and $\sin(\theta_{j2} - \theta_{12})$, $j = 2, 3$ are weighed by the first row of the coupling matrices P, Q , namely, p_{11}, p_{12}, q_{11} , and q_{12} , then summed to determine frequency $\dot{\theta}_{11}$. The second row of the matrices, in a similar manner, would be contributing to the dynamics on the θ_{i2} dimension.

we propose a novel interacting mechanism, the matrix coupling, that directly operates on the differences of the angle variables for the oscillators on the unit sphere, and report phase transitions as well as other systematical behaviors that distinguish from other high-dimensional Kuramoto generalizations. The proposed dynamics reads

$$\dot{\theta}_i = \begin{bmatrix} \dot{\theta}_{i1} \\ \dot{\theta}_{i2} \end{bmatrix} = \begin{bmatrix} \omega_{i1} \\ \omega_{i2} \end{bmatrix} + \frac{1}{N} \cdot A \sum_{j=1}^N \mathbf{sin}(\theta_j - \theta_i) \quad (1)$$

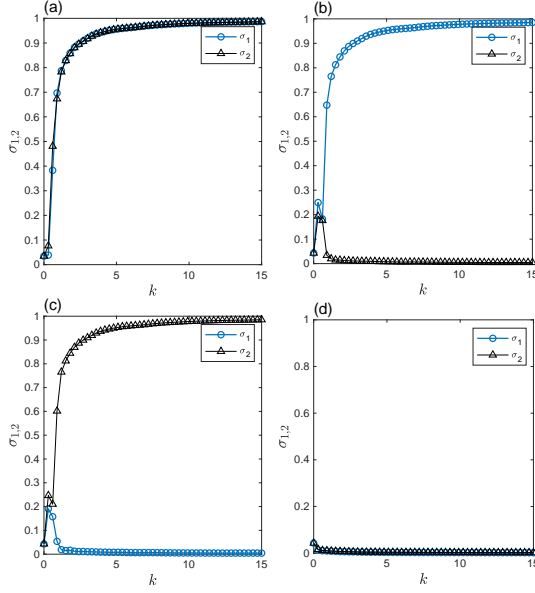


FIG. 2. *Transitions of $\sigma_{1,2}$ under candidate matrices A_i .* Panels (a), (b), (c), and (d) are results of direct simulation of eqn. (1) on $N = 1000$ oscillators with $A_i = A_1, A_2, A_3, A_4$ respectively; each panel demonstrates the values of the order parameter σ_1 (blue circle) and σ_2 (black triangle) during the transition under the corresponding candidate matrix, for which $\sigma_1 \rightarrow 1 (\sigma_2 \rightarrow 1)$ indicates a high level of synchrony in dimension $\theta_{i1} (\theta_{i2})$ while $\sigma_1 \rightarrow 0 (\sigma_2 \rightarrow 0)$ indicates desynchrony, i.e., a uniform distribution in dimension $\theta_{i1} (\theta_{i2})$.

where both the dimensions θ_{i1}, θ_{i2} are assumed to be angular variables of oscillator i , with ω_{i1} and ω_{i2} drawn from the distributions $g_1(\omega_1)$ and $g_2(\omega_2)$ being their natural frequencies of oscillation in that direction. Now, instead of the averaged scalar factor, we consider an averaged, all-to-all coupling with the matrix $A = \begin{bmatrix} a_{11} & a_{12} \\ a_{21} & a_{22} \end{bmatrix} \in \mathbb{R}^{2 \times 2}$, that acts on the sum of vectors $[\sin(\theta_{j1} - \theta_{i1}) \sin(\theta_{j2} - \theta_{i2})]^T$. The matrix coupling arises naturally from the characterization of the inter-dimensional communication amongst multi-dimensional entities, and has been considered in the context of opinion dynamics on interdependent topics [13], synchronization on coupled arrays of LC oscillators or pendulums [14] and more [15, 16]. FIG. 1 illustrates the mechanism of the two-dimensional Kuramoto model with the matrix-coupling; one should notice that the dynamics on one dimension of a specific oscillator is taking direct influences from both dimensions of the neighboring oscillators, except the dimensions are weighed differently by the row elements. This interaction is further clarified if we define the complex order parameters for the two dimensions as $\rho_1 = \frac{1}{N} \sum_{j=1}^N e^{i\theta_{j1}} = \sigma_1 e^{i\Psi_1}$, $\rho_2 = \frac{1}{N} \sum_{j=1}^N e^{i\theta_{j2}} = \sigma_2 e^{i\Psi_2}$, where $0 \leq \sigma_{1,2} \leq 1$ and $\Psi_{1,2}$ denote the average phases; the equations of motion for θ_{i1}, θ_{i2} are then

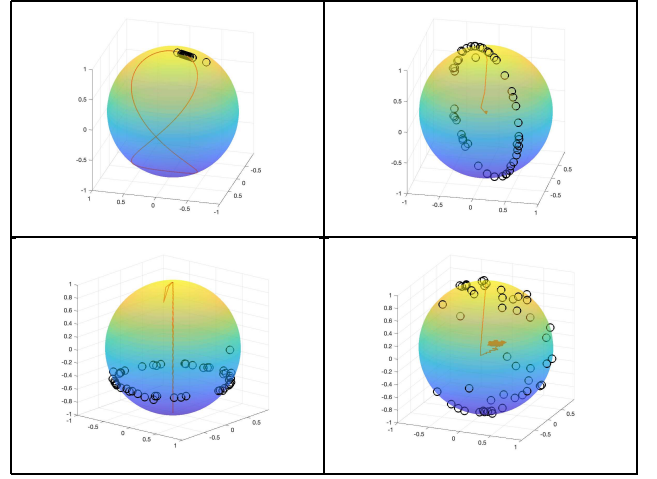


FIG. 3. *Visualization on the unit sphere.* Take θ_{i1} as the azimuthal angle and θ_{i2} as the polar angle, the population of oscillators (black circles) are projected onto the surface of a unit sphere, where the orange line stands for the trajectory of the average position of the population w.r.t time. We illustrate with $N = 50$ oscillators whose initial conditions are identically $\theta_i(0) = \mathbf{0}$. The four panels correspond to the four modes the system eventually settled in with the candidate matrices A_1, A_2, A_3, A_4 , as k is tuned to 50. The upper-left panel shows when the oscillators are fully synchronized (in frequency) on both θ_{i1} and θ_{i2} dimensions; the oscillators remain relatively static and travel along the orange orbit at a constant speed. Upper-right panel shows when the oscillators are only θ_{i1} synchronized and stay disarranged on the ring that rotates uniformly about the z -axis, their average position soon approaching the origin. In the lower-left panel where the population is only θ_{i2} synchronized, the majority distributes on a ring that is shrinking and stretching as it moves up and down in the z -direction. While for the lower-right panel, the θ_{i1}, θ_{i2} desynchronized oscillators drift across the surface and do not form any groups or show any particular pattern. We mention, in the first three cases, the velocity of the mean-field is visibly non-zero because of the limitation of N , which renders the center of the natural frequencies to be non-zero.

$$\begin{aligned} \dot{\theta}_{i1} &= \omega_{i1} - a_{11}\sigma_1 \sin(\theta_{i1} - \Psi_1) - a_{12}\sigma_2 \sin(\theta_{i2} - \Psi_2), \\ \dot{\theta}_{i2} &= \omega_{i2} - a_{21}\sigma_1 \sin(\theta_{i1} - \Psi_1) - a_{22}\sigma_2 \sin(\theta_{i2} - \Psi_2). \end{aligned} \quad (2)$$

We see that the instantaneous frequencies are modulated by the weighed θ_{i1} mean-field and θ_{i2} mean-field. It is then of question what the variation of the elements is going to bring to the state of the system, measured by the order parameters ρ_1, ρ_2 .

To get down to the essentials, we simulate on $N = 1000$ oscillators whose initial conditions are identically $\theta_i(0) = \mathbf{0}$, assuming the natural frequencies $\omega_{i1} = \omega_{i2}$ to be drawn from the Lorentzian distribution $g_1(\omega) = g_2(\omega) = g(\omega) = \frac{1}{\pi} \frac{\gamma}{(\omega - \Omega)^2 + \gamma^2}$ with symmetry center $\Omega = 0$ and spread $\gamma = 1$.

The first discovery could be exemplified by four can-

candidate matrices A_1, A_2, A_3, A_4 we used to generate FIG. 2, where $A_1 = \begin{bmatrix} 4.27 & 0.11 \\ 7.42 & 3.20 \end{bmatrix}$, $A_2 = \begin{bmatrix} 3.80 & 7.54 \\ 7.57 & 2.86 \end{bmatrix}$, $A_3 = \begin{bmatrix} 2.86 & 7.54 \\ 7.57 & 3.80 \end{bmatrix}$, $A_4 = \begin{bmatrix} -24.11 & 6.28 \\ 6.27 & -17.89 \end{bmatrix}$. For the experiment, let $A = kA_i, i \in \{1, 2, 3, 4\}$, we adiabatically increase k from 0 to 15 with increment $\Delta k = 0.3$ and calculate the average of $\rho_{1,2}$ during a set period of time as the stationary order parameters of the corresponding k . We note that this scaling is fundamentally different from that in other generalized models, as there are now four independent variables undergoing changes in the parameter space of the system. FIG. 2 reports our result that for A_1 and A_4 , both the θ_{i1} dimension and the θ_{i2} dimension go through qualitatively similar transitions either from being largely desynchronized to a complete frequency synchronization ($\sigma_{1,2} \rightarrow 1$), or to a complete desynchronization ($\sigma_{1,2} \rightarrow 0$). Yet for A_2 and A_3 whose diagonal elements are interchanged, the transitions on θ_{i1} dimension and θ_{i2} dimension go to opposite directions, i.e., $\sigma_1 \rightarrow 1, \sigma_2 \rightarrow 0$ or $\sigma_1 \rightarrow 0, \sigma_2 \rightarrow 1$ as the elements of A are simultaneously and sufficiently increased.

One thing to extract from these experiments is that, the matrix coupling enables the multi-dimensional Kuramoto oscillators to separate the transition to synchronization/desynchronization in different dimensions, which has not been seen in other high-dimensional generalizations [11, 12]. Depicting the combinations of $\sigma_{1,2}$ on the unit sphere, FIG. 3 shows how the system sets into four qualitatively different modes of distribution and motion with the configurations of A_i . As to how the proposed model is able to achieve this, we mention, which confirms the results by many other choices of A_i , that the positivity/negativity of the two real eigenvalues $\lambda_{1,2}$ of A is reflected on $\sigma_{1,2}$ for $k > 0$ sufficiently large. Demonstrating this with the candidate matrices, for A_1 with $\lambda_{1,2} \geq 0$, the order parameters has $\sigma_{1,2} \rightarrow 1$, while for A_4 with $\lambda_{1,2} \leq 0$ there is $\sigma_{1,2} \rightarrow 0$ (note that only one of λ_1, λ_2 is permitted to be zero); meanwhile for A_2 and A_3 that satisfy $\lambda_1 \cdot \lambda_2 < 0$, one obtains $\sigma_1 \rightarrow 1, \sigma_2 \rightarrow 0$ or $\sigma_1 \rightarrow 0, \sigma_2 \rightarrow 1$. When the elements of the coupling matrix are altered in this manner, the transition in dimension θ_{i1} or θ_{i2} experiences several minor jumps according to $\sigma_{1,2}$ even for populations as large as $N = 1000$, which has to do with the contribution of the drifting oscillators to the order parameters. But in all, the transition is comparable to that of the second-order. With the disposition of the positivity/negativity of the eigenvalues of the coupling matrix, the system has the tendency to set into the four modes with complete synchronization/desynchronization of the two dimensions. This does not apply, however, when the coupling matrix A_i satisfies $a_{11} = a_{22} > 0, a_{12} = a_{21}$, as we have also discovered that for this kind of weight matrix, the positively increased

k only generates transition of $\sigma_1 \rightarrow 1, \sigma_2 \rightarrow 1$. Another intricacy arises when the eigenvalues $\lambda_{1,2}$ are a conjugate pair, which according to our experiments, distinguishes between $|Re(\lambda)| > 1$ and $|Re(\lambda)| \leq 1$. While the case of $|Re(\lambda)| > 1$ much resembles that where the eigenvalues are real, which means $\sigma_{1,2} \rightarrow 1$ as $Re(\lambda_{1,2}) > 1$ and $\sigma_{1,2} \rightarrow 0$ as $Re(\lambda_{1,2}) < -1$, the case of $|Re(\lambda)| \leq 1$ gets more eccentric and always ends up with $\sigma_{1,2}$ settling into steady values significantly between 0 and 1. For the remaining of this work, we avert our attention from these ramifications and focus on the coupling matrices that are well-behaved with real eigenvalues that lead to a full synchronization/desynchronization on the two dimensions.

Our second discovery emerges from the four modes exhibited that lead to the inevitable question of if the system is actually capable of switching between one mode to another by modulating the elements of A , as there are obviously many ways the coupling matrix A could alter to produce dynamics apart from being steadily scaled by a factor k . What we then do is to encode the system modes into binary digits 00, 01, 10, 11 encouraged by the combination of $\sigma_{1,2}$ and find representative matrices M_1, M_2, M_3, M_4 for these modes, which means kM_i let the system set into mode 00/01/10/11 with k positive and sufficiently large, and with a uniform initial condition $\theta_i(0) = \mathbf{0}$.

For the experiment, we demonstrate the switchings on $N = 100$ oscillators whose natural frequencies $\omega_{i1} = \omega_{i2} = \omega_i$ are drawn from the standard Lorentzian distribution. Specifically, the representative matrices are $M_1 = \begin{bmatrix} -16 & -10 \\ -10 & -20 \end{bmatrix}$ for mode 00, $M_2 = \begin{bmatrix} 16 & 30 \\ 30 & 20 \end{bmatrix}$ for mode 01, $M_3 = \begin{bmatrix} 16 & 30 \\ 30 & -4 \end{bmatrix}$ for mode 10, $M_4 = \begin{bmatrix} 16 & 10 \\ 10 & 20 \end{bmatrix}$ for mode 11, that will be morphing into one another during the switching process. For each switching in (a)~(l) in FIG. 4., we simulate under dynamics (1) from $\theta_i(0) = \mathbf{0}$ and $A = M_i$ and break down its transition to $A = M_j$ into 51 steps, $i, j \in \{1, 2, 3, 4\}$; for each step, an average of the steady state order parameters over time is evaluated as a data point on figures (a)~(l), and the overall results of $\sigma_{1,2}$ are displayed in FIG. 4. For switchings (a) to (l) other than (d), we use linear interpolation in the 51 steps to compensate the difference between the matrices, i.e.,

$$M^{s+1} = M^s + \Lambda \quad (3)$$

where $\Lambda = (M_j - M_i)/50$ is the incremental matrix so that $M^0 = M_i = \begin{bmatrix} a_{11}^i & a_{12}^i \\ a_{21}^i & a_{22}^i \end{bmatrix}$, $M^{50} = M_j = \begin{bmatrix} a_{11}^j & a_{12}^j \\ a_{21}^j & a_{22}^j \end{bmatrix}$. However for (d) which is from 10 to 01, the switching does not happen with direct interpolation between $M_3 = \begin{bmatrix} 16 & 30 \\ 30 & -4 \end{bmatrix}$ and $M_2 = \begin{bmatrix} 16 & 30 \\ 30 & 20 \end{bmatrix}$; actually, one needs

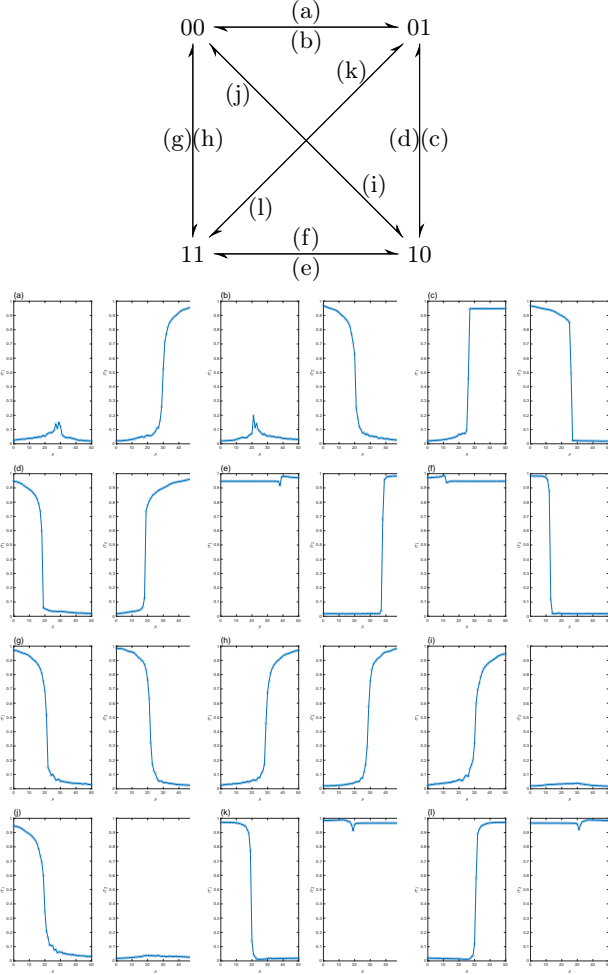


FIG. 4. *Switching diagram of $\sigma_{1,2}$.* The diagram on the top illustrates the combination of σ_1 and σ_2 and their interchanging process indexed as (a) to (l). Figures below draw separately the transitions of σ_1 and σ_2 in the aforementioned (a) to (l) with respect to step s as in eqn. (3). Refer to the text for the configuration of the experiment.

to extend the increasing of a_{22} till around 31 to induce the switching. Therefore for (d), we first evenly decrease a_{11} while increasing a_{22} of M_3 to $\begin{bmatrix} 0 & 30 \\ 30 & 8 \end{bmatrix}$ in 26 steps, then increase evenly both a_{11} and a_{22} in the remaining steps to M_2 which has allowed the desired switching from 10 to 01. FIG. 4. verifies that, as the representative matrix M_i morphs into M_j in the twelve scenarios, the system completes a switching from M_i 's corresponding mode to that of M_j 's with either continuous transitions or explosive transitions to synchronization/desynchronization. Although we have not touched on the problem of initial conditions in this work, consecutive switchings with different combinations of (a)~(l) are produced as we continue to apply interpolation, and obtain a sequence of $\sigma_{1,2}$ that are ultimately varying with time, which might

be a suggestion that the alternating synchronization and desynchronization in the different dimensions of the oscillators display capacity in coding information in a binary fashion under specific choices of the coupling matrix.

To shed light on the phenomenon observed, we employ a self-consistency analysis where the steady state assumption guarantees that $\dot{\Psi}_1 = \Omega_1$, $\dot{\Psi}_2 = \Omega_2$, with $\Omega_{1,2}$ being the symmetry centers of $g_1(\omega_1)$ and $g_2(\omega_2)$. Thus by introducing the rotating frame $\psi_{i1} = \theta_{i1} - \Omega_1 t$, $\psi_{i2} = \theta_{i2} - \Omega_2 t$, eqn. (2) now turns into

$$\begin{aligned} \dot{\psi}_{i1} &= (\omega_{i1} - \Omega_1) - (a_{11}\sigma_1 \sin \psi_{i1} + a_{12}\sigma_2 \sin \psi_{i2}), \\ \dot{\psi}_{i2} &= (\omega_{i2} - \Omega_2) - (a_{21}\sigma_1 \sin \psi_{i1} + a_{22}\sigma_2 \sin \psi_{i2}). \end{aligned} \quad (4)$$

Eqn. (4) suggests that when either of the order parameters $\sigma_{1,2}$ is at the proximity of zero, e.g., when $\sigma_2 \approx 0$, the other dimension of the oscillators get decoupled from its influence and reduces to the dynamic of the classic Kuramoto model, that is in our example, $\dot{\psi}_{i1} = (\omega_{i1} - \Omega_1) - a_{11}\sigma_1 \sin \psi_{i1}$, and $\dot{\psi}_{i2}$ being driven by the external field $\sigma_1 \sin \psi_{i1}$. Another simplified scenario is when the system is devoid of desynchronized oscillators on both dimensions as in the case (f) of FIG. 4., where A is invertible and $\sigma_{1,2} \approx 1$ at the beginning of the transition. Denote $A^{-1} = \begin{bmatrix} b_{11} & b_{12} \\ b_{21} & b_{22} \end{bmatrix}$; for ψ_{i1} and ψ_{i2} to have their respective attractors at the same time, the synchronization domains are

$$\begin{aligned} D_1 &= \left\{ (\omega_{i1}, \omega_{i2}) : \left| \frac{b_{11}(\omega_{i1} - \Omega_1) + b_{12}(\omega_{i2} - \Omega_2)}{\sigma_1} \right| < 1 \right\}, \\ D_2 &= \left\{ (\omega_{i1}, \omega_{i2}) : \left| \frac{b_{21}(\omega_{i1} - \Omega_1) + b_{22}(\omega_{i2} - \Omega_2)}{\sigma_2} \right| < 1 \right\}. \end{aligned} \quad (5)$$

Solve for $\dot{\psi}_{i1} = 0$ and $\dot{\psi}_{i2} = 0$, the fixed point for vector $[\psi_{i1} \ \psi_{i2}]$ is $\psi_{i1}^* = \arcsin\left(\frac{b_{11}(\omega_{i1} - \Omega_1) + b_{12}(\omega_{i2} - \Omega_2)}{\sigma_1}\right)$, $\psi_{i2}^* = \arcsin\left(\frac{b_{21}(\omega_{i1} - \Omega_1) + b_{22}(\omega_{i2} - \Omega_2)}{\sigma_2}\right)$ for $D_1 \cap D_2 \neq \emptyset$; under the premise that $\omega_{i1} = \omega_{i2}$, these expressions can be further simplified with $\Omega_1 = \Omega_2 = \Omega$. Since both $\dot{\psi}_{i1}$ and $\dot{\psi}_{i2}$ are synchronized before the abrupt desynchronization, we calculate only synchronized contribution to the order parameters $\sigma_{1,2}$. Apply the coordinate transformation $\sin \Delta_1 = \frac{a_{22} - a_{12}}{|A|\sigma_1}(\omega_1 - \Omega)$, $\sin \Delta_2 = \frac{a_{11} - a_{21}}{|A|\sigma_2}(\omega_2 - \Omega)$, we then need to decide the new synchronization domain $D_1 \cap D_2 = \{(\Delta_1, \Delta_2) : -\eta_1 < \Delta_1 < \eta_1, -\eta_2 < \Delta_2 < \eta_2\}$ under this coordinate for $\omega_1 = \omega_2$. In the continuum limit $N \rightarrow \infty$, the order parameters are obtained as

$$\begin{aligned} \sigma_1 \left\{ 1 - \left| \frac{|A|}{a_{22} - a_{12}} \right| \int_{-\eta_1}^{\eta_1} \cos^2 \Delta_1 g(\Omega) + \frac{|A|\sigma_1}{a_{22} - a_{12}} \sin \Delta_1 \right. \\ \left. \cdot d\Delta_1 \right\} &= 0, \\ \sigma_2 \left\{ 1 - \left| \frac{|A|}{a_{11} - a_{21}} \right| \int_{-\eta_2}^{\eta_2} \cos^2 \Delta_2 g(\Omega) + \frac{|A|\sigma_2}{a_{11} - a_{21}} \sin \Delta_2 \right. \\ \left. \cdot d\Delta_2 \right\} &= 0, \end{aligned} \quad (6)$$

for which when $\left| \frac{\sigma_1}{a_{22}-a_{12}} \right| < \left| \frac{\sigma_2}{a_{11}-a_{21}} \right|$, there is $\eta_1 = \frac{\pi}{2}, \eta_2 = \arcsin\left(\left| \frac{a_{11}-a_{21}}{a_{22}-a_{12}} \right| \frac{\sigma_1}{\sigma_2}\right)$; alternatively when $\left| \frac{\sigma_1}{a_{22}-a_{12}} \right| > \left| \frac{\sigma_2}{a_{11}-a_{21}} \right|$, there is $\eta_1 = \left(\arcsin\left(\left| \frac{a_{11}-a_{21}}{a_{22}-a_{12}} \right| \frac{\sigma_1}{\sigma_2}\right)\right)^{-1}, \eta_2 = \frac{\pi}{2}$. Note that the integrated function is always positive, thus normally, apart from the uniformly distributed solution $\sigma_1 = \sigma_2 = 0$, there exists another steady state solution suppose $\left| \frac{|A|}{a_{22}-a_{12}} \right| \neq 0, \left| \frac{|A|}{a_{11}-a_{21}} \right| \neq 0$. This explains the abrupt transition to the desynchronized state for σ_2 , since when $\left| \frac{|A|}{a_{11}-a_{21}} \right|$ is gradually tuned to zero, the partially synchronized solution for σ_2 vanishes and momentarily leaves $\sigma_2 = 0$ as the only solution for the system. Actually, from the perspective of the synchronization domains, the explanation covers a wider range of phenomena in FIG. 4. for which with $\omega_1 = \omega_2 = \omega$, the integration domain is equivalently $D_1 \cap D_2, D_1 : |\omega - \Omega| < \frac{\sigma_1 |A|}{|a_{22}-a_{12}|}, D_2 : |\omega - \Omega| < \frac{\sigma_2 |A|}{|a_{11}-a_{21}|}$, that is, $D_1 \cap D_2 = \{\omega : |\omega - \Omega| < \min\left\{\left| \frac{|A|}{a_{22}-a_{12}} \right|, \left| \frac{|A|}{a_{11}-a_{21}} \right| \right\}\}$. For (f), $\frac{|A|}{a_{11}-a_{21}}$ passes from being positive to being negative one step earlier than $\frac{|A|}{a_{22}-a_{12}}$ and the right side of the expression D_2 approaches closely to zero, which means almost all the oscillators other than those with natural frequencies $\omega_{i1} = \omega_{i2} = \Omega$ are not entrained by the mean-field of the second dimension, thus the order parameter σ_2 has to see a significant drop. Indeed, for switchings (a)~(l) other than (c), we have observed for D_1 and D_2 to cross zero almost simultaneously, and the narrower domain eventually dominates the transition to synchronization, i.e., $\sigma_1 \rightarrow 1$ if $D_1 \subset D_2$ at the end of the transition.

In this Letter, we present a novel coupling mechanism with the 2×2 real matrices on the two-dimensional Kuramoto oscillators and uncover distinct phenomena it induces with different configurations and variations of the coupling matrix. One thing we have discovered is that, the positivity or negativity of the eigenvalues of the matrix indicates the tendency of the two dimensions of the oscillators to set into synchronization or desynchronization, as the four elements of the matrix are scaled by a positive factor sufficiently large. Since the synchronization and desynchronization of the two dimensions are separated, their combinations suggest four qualitatively distinct modes of the system that are possible to switch between one and another through the variations of the

coupling matrix. The switching between synchronization and desynchronization in the two dimensions with respect to time displays potential in information coding and memory storage [17] and imitates other phenomenology in biology like the unihemispheric slow-wave sleep of dolphins [18], where the two hemispheres of the dolphin alternate between resting and waking during its sleep, the two behaviors existing independently at the same time. Apart from the experiments with 2×2 real matrices presented in this work, we have also simulated on 3×3 real matrices with various eigenvalue arrangements and recovered the potential eight combinations of the order parameters $\sigma_{1,2,3}$, suggesting the proposed model to be quite generalizable into even higher dimensions.

* dwli@sjtu.edu.cn

- [1] A. T. Winfree, *Journal of theoretical biology* **16**, 15 (1967).
- [2] N. Wiener, *Cybernetics or Control and Communication in the Animal and the Machine* (MIT press, 2019).
- [3] S. Watanabe and S. H. Strogatz, *Physica D: Nonlinear Phenomena* **74**, 197 (1994).
- [4] Y. Kuramoto, *Chemical oscillations, waves, and turbulence* (Courier Corporation, 2003).
- [5] S. H. Strogatz, *Physica D: Nonlinear Phenomena* **143**, 1 (2000).
- [6] J. Van Hemmen and W. Wreszinski, *Journal of Statistical Physics* **72**, 145 (1993).
- [7] T. Uezu, T. Kimoto, S. Kiyokawa, and M. Okada, *Journal of the Physical Society of Japan* **84**, 033001 (2015).
- [8] J. Buck and E. Buck, *Science* **159**, 1319 (1968).
- [9] J. A. Acebrón, L. L. Bonilla, C. J. P. Vicente, F. Ritort, and R. Spigler, *Reviews of modern physics* **77**, 137 (2005).
- [10] J. Zhu, *Physics Letters A* **377**, 2939 (2013).
- [11] S. Chandra, M. Girvan, and E. Ott, *Physical Review X* **9**, 011002 (2019).
- [12] X. Zhang, S. Boccaletti, S. Guan, and Z. Liu, *Physical review letters* **114**, 038701 (2015).
- [13] N. E. Friedkin, A. V. Proskurnikov, R. Tempo, and S. E. Parsegov, *Science* **354**, 321 (2016).
- [14] S. E. Tuna, *Automatica* **107**, 154 (2019).
- [15] M. H. Trinh, C. VanÁ Nguyen, Y.-H. Lim, and H.-S. Ahn, *Automatica* **89**, 415 (2018).
- [16] S. Zhao and D. Zelazo, *Automatica* **69**, 334 (2016).
- [17] J. Fell and N. Axmacher, *Nature reviews neuroscience* **12**, 105 (2011).
- [18] L. Mukhametov, A. Y. Supin, and I. Polyakova, *Brain research* (1977).